DOI: 10.1002/anie.200905359

Hydrogen Storage

Methylguanidinium Borohydride: An Ionic-Liquid-Based Hydrogen-Storage Material**

*Amir Doroodian, Joachim E. Dengler, Alexander Genest, Notker Rösch, and Bernhard Rieger**

Hydrogen is increasingly being considered as a “clean” alternative to fossil fuels.[1] A challenge for the application of hydrogen in on-board transportation systems is the development of efficient chemical hydrogen-storage materials that can allow hydrogen release to occur reversibly under the operation conditions. Ammonia borane (NH_3BH_3) which has a high hydrogen-storage capacity (19.6 wt %) has been investigated intensively.[2–11]

To date there is relatively little work that exploits the advantageous features of ionic liquids—low vapor pressure, high density, and low viscosity—in combination with hydrogen storage.[12]

Herein we present methylguanidinium borohydride $(N_3H_8C)C^+BH_4^-$ (**1**) an ionic liquid (m.p. $-5\,^\circ C$, density $\varrho(20\,^\circ C) = 0.95\ g\,mL^{-1}$), which releases 9.0 wt % H_2 under both thermal and catalytic conditions. To our knowledge, **1** is the first ionic liquid with effective hydrogen-storage capacity.

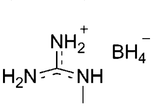

1

The ionic liquid is compared with guanidinium borohydride $(N_3H_6)C^+BH_4^-$ (**2**), which with 10.7 wt % hydrogen has potential as a hydrogen source.

The preparation of **2** by ion exchange between $Ca(BH_4)_2$ and guanidinium carbonate in water, or by reaction of $NaBH_4$ and guanidinium sulfate in isopropanol, respectively, has been already detailed by Titov et al.[13,14] An alternative metathesis-based method for the preparation of **1** and **2** is presented herein. To prepare **2** guanidinium chloride is mixed with sodium borohydride in THF at 0 °C affording two discrete phases; the upper phase consisting of THF, the lower phase comprising guanidinium borohydride with 2.5 equivalents of THF (as determined by NMR spectroscopy, CD_2Cl_2 external standard). Removal of volatile components under vacuum affords **2** as a white solid. The same approach was used for the preparation of **1**, mixing THF slurries of methylguanidine hydrochloride and sodium borohydride at room temperature affords **1** as a yellow viscous liquid. The molecular structure of **2** comprises BH_4^- and $(NH_2)_3C^+$ ions connected by dihydrogen bonds.[15]

The kinetic dehydrogenation studies of **1** and **2** were performed in homogeneous diglyme solution and the evolved hydrogen was measured volumetrically. The rate of hydrogen evolution depends on the temperature, concentration, and nature of catalyst (Figure 1).

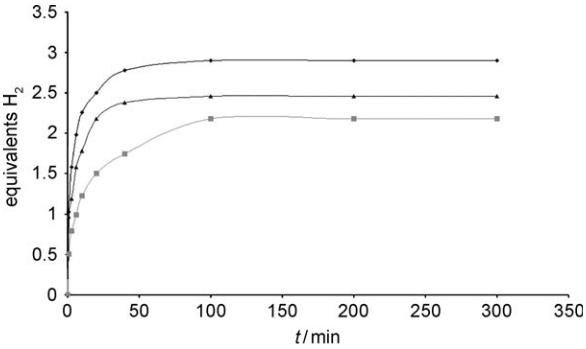

Figure 1. Kinetics of catalytic (Wilkinson catalyst, $FeCl_2$) and thermal dehydrogenation of **1**. ◆ Wilkinson catalyst, ▲ $FeCl_2$, ■ thermal decomposition.

During the gradual dehydrogenation of **1** a white precipitate was formed from the yellow solution. The kinetic measurements in homogenous diglyme solution at 75 °C show the evolution of 2.9 equivalents of hydrogen for Wilkinson’s catalyst and 2.4 equivalents for $FeCl_2$ (both within 20 min; Table 1). By coupling of hydride and proton theoretically four equivalents of H_2 can be released, which leads to the formation of B−N bonds (B−N dehydrocoupling).

The amount of hydrogen evolved from **2** in dry diglyme at 75 °C by loading with Wilkinson’s and $FeCl_2$ catalyst equates to 3.9 (10.3 wt %) and 2.0 (5.3 wt %) equivalents, respectively. This result suggests that quantitative H_2 evolution and higher dehydrogenation rates for **1** using improved catalysts may be achieved. However the observed dehydrogenation rates demonstrated are still insufficient for practical application.

Table 1: Amount of hydrogen gas evolved from **1** with catalysts.

Catalyst	*T*	Equiv H_2
Wilkinson’s cat. (1 mol %)	75 °C	2.9
$FeCl_2$ (1 mol %)	75 °C	2.4
thermal	75 °C	2.3

---

[*] A. Doroodian, J. E. Dengler, Prof. B. Rieger
Technische Universität München
WACKER-Lehrstuhl für Makromolekulare Chemie
Lichtenbergstrasse 4, 85747 Garching (Germany)
Fax: (+49) 89-2891-3571
E-mail: rieger@tum.de
Homepage: http://www.makro.ch.tum.de/

A. Genest, Prof. N. Rösch
Technische Universität München, Department Chemie
Lichtenbergstrasse 4, 85747 Garching (Germany)

[**] Thanks to Dr. G. Raudaschl-Sieber for supporting solid-state 11B NMR spectra. Thanks to Dr. S. Vagin and Dr. C. Anderson for cooperation during preparation of this paper.

Supporting information for this article is available on the WWW under http://dx.doi.org/10.1002/anie.200905359.

Thermal gravimetric analysis (TGA) and differential scanning calorimetry (DSC) measurements of **2** have been presented by Groshens and Hollins.[15b] TGA-MS analysis of **1** and **2** shows a 10.84 % (theoretical dehydrocoupling: 8.97 %)[16] and 10.64 % (theoretical dehydrocoupling: 10.65 %) weight loss reached in the temperature range between 40 °C and 180 °C, accompanied by a shoulder up to 200 °C, which can not be assigned to a dehydrocoupling process. The purity of evolved gas has been established by MS analysis in the range of 2 g mol^{-1} to 60 g mol^{-1} using TGA-MS coupling, which indicates hydrogen as the predominant product. In the temperature range 40 °C to 120 °C ammonia was below the not detected for both **1** and **2** in the evolved gas stream (Figure 2). Upon further heating of the compounds, traces of ammonia were detected in the 120 °C to 580 °C temperature range in both cases (indicating the onset of decomposition), however the mass loss observed for both **1** and **2** is continuous (release of larger molecules $m/z > 60$) until complete decomposition of the compounds is reached (approximately 800 °C).

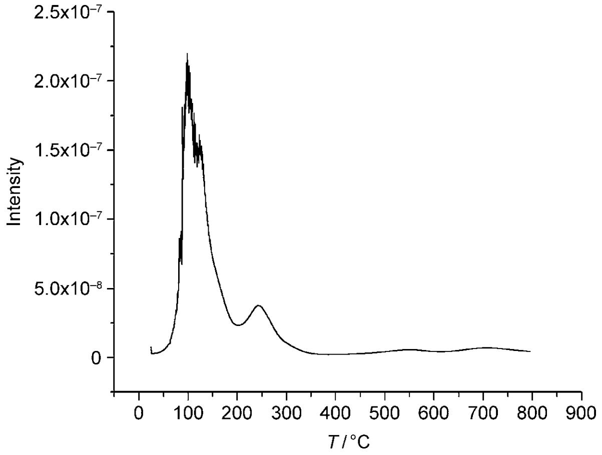

Figure 2. Evolution of hydrogen gas from **1** as detected by TGA-MS.

The DSC curve of **1** demonstrates two exothermic processes which are connected by an endothermic process at 80 °C (Supporting Information). It is tentatively proposed that the exothermic H_2 evolution is superimposed with several phase transitions processes, from which only the feature at 80 C is seen. The enthalpy contributions of these phase transitions are not easy to compensate. The overall liberated energy (ΔQ) for **1** over the range 20 °C to 200 °C is determined by integration of the DSC curves to be $-85\ \text{kJ mol}^{-1}$. For the thermal decomposition of **2**, also between 20 °C to 200 °C, $\Delta Q = -67\ \text{kJ mol}^{-1}$.

The thermal dehydrogenation of **1** and **2** were broadly similar with the continuous precipitation of a white solid from the diglyme solution over the course of the reactions. The solution phase contains residual guanidinium borohydrides in both cases (determined by NMR spectroscopy).

The insoluble products obtained from the dehydrogenation of **1** and **2** were characterized with the aid of solid-state ^{11}B magic-angle spinning (MAS) NMR spectroscopy. The solid-state ^{11}B MAS NMR spectrum of the precipitate from the thermal and catalytic dehydrogenation of **1** exhibits signals at $\delta = -38$, -27, -15, -1, and 10 ppm. The ^{11}B MAS NMR spectrum of the precipitate from the dehydrogenation of **2** shows similar shifts. The three products of catalytic and thermal decomposition each show two principle signals at around $\delta = -39$ and -4 ppm with a shoulder at $\delta = -7$ ppm (Figure 3). Minor signals appear at $\delta = -28$, -16, and $+9$ ppm. The spectra differ only by the relative intensity of the observed signals.

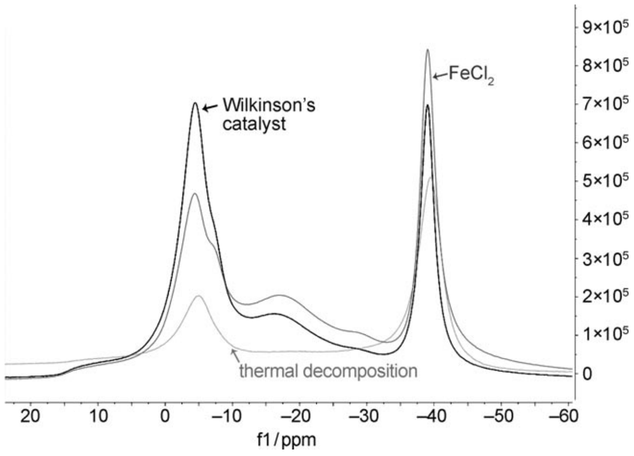

Figure 3. ^{11}B solid-state NMR spectra of the decomposition products of **2** by thermal (75 °C), iron-catalyzed (2 mol % catalyst, 75 °C), and rhodium-catalyzed (Wilkinson's catalyst, 0.1 mol % catalyst, 75 °C) dehydrogenation.

The chemical shifts in the ^{11}B spectrum were calculated for **2** (the signal intensity is better and the calculations are simpler than for **1**). The calculated spectrum was compared with the observed ^{11}B NMR spectroscopic shifts of **1** and **2**. Although **2** lacks a methyl group, this substituent has a minimal effect on the observed chemical shifts, thus enabling comparisons.

The solid-state ^{13}C NMR spectrum of **1** exhibits two signals, assigned to the guanidinium moiety at $\delta = +159$ ppm and the methyl group at $\delta = +28$ ppm (Supporting Information). The latter indicates no appreciable change in the carbon character during the dehydrogenation reaction.

Figure 4 summarizes the results of RI-MP2/GIAO calculations on the ^{11}B NMR chemical shift (Turbomole, TZVP basis set)[17,18] of possible dehydrocoupling products of **2**. Calculations with a comparable method had already been successfully employed for predicting ^{11}B NMR spectra.[19] The sharp signals at $\delta = -39$ ppm are attributed to residual BH_4^-, which remains in the product mixture. The second signal at $\delta = -4$ ppm with a shoulder at $\delta = -8$ ppm is assigned to tetravalent borane nitrogen substances whose shift increases with the number of coordinated nitrogen atoms, from $\delta = -8.5$ ppm for two, to $\delta = -6.0$ ppm for three, and to $\delta = -3.5$ ppm for four bound guanidinium units (Figure 4 b,c). The calculations show a signal at $\delta = -19.4$ ppm for a single guanidinium unit coordinated to BH_3 (Figure 4 a). The calculated results are 1–3 ppm higher than the measured

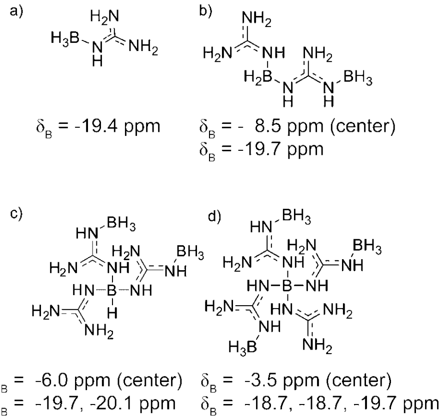

Figure 4. Calculated ^{11}B NMR chemical shifts for proposed structures that arise from dehydrogenation of **2**

signals. Therefore the calculated value of −19.4 ppm would correspond to measured signals between −20.4 and −22.4 ppm, and hence it cannot be assigned to the band at −16 ppm. As all species with several guanidinium units contain terminal BH_3 groups with different chemical environments, the broad bands between −16 and −24 ppm can be rationalized in this way (see Figures 3 and 4 c,d).

The ESI-MS characterization of the solid dehydrogenation products from compounds **1** and **2** was performed in warm isopropanol. It is assumed that the improved solubility over time, in both cases, is a direct result of hydrolysis of the oligomeric products. The predominant formation of dimeric or trimeric boron-bridged species is in accordance with branched oligomers as dehydrocoupling products.

Thermal or catalytic decomposition of compounds **1** and **2**, in contrast to that of ammonia borane, affords a series of well defined, solid products. Their high capacity to release pure H_2 makes these compounds interesting targets for hydrogen storage applications.

Received: September 24, 2009
Revised: November 24, 2009
Published online: February 9, 2010

Keywords: ab initio calculations · boranes · energy carriers · hydrogen storage · ionic liquids

[1] S. Satyapal, J. Petrovic, C. Read, G. Thomas, G. Ordaz, *Catal. Today* **2007**, *120*, 246 – 256.

[2] T. B. Marder, *Angew. Chem.* **2007**, *119*, 8262 – 8264; *Angew. Chem. Int. Ed.* **2007**, *46*, 8116 – 8118, and references therein.

[3] W. T. Klooster, T. F. Koetzle, E. M. Siegbahn, T. B. Richardson, R. H. Crabtree, *J. Am. Chem. Soc.* **1999**, *121*, 6337 – 6343.

[4] R. J. Keaton, J. M. Blacquiere, R. T. Baker, *J. Am. Chem. Soc.* **2007**, *129*, 1844 – 1845.

[5] A. Paul, C. B. Musgrave, *Angew. Chem.* **2007**, *119*, 8301 – 8304; *Angew. Chem. Int. Ed.* **2007**, *46*, 8153 – 8156.

[6] X. Yang, M. B. Hall, *J. Am. Chem. Soc.* **2008**, *130*, 1798 – 1799.

[7] a) C. A. Jaska, K. Temple, A. J. Lough, I. Manners, *Chem. Commun.* **2001**, 962 – 963; b) C. A. Jaska, K. Temple, A. J. Lough, I. Manners, *J. Am. Chem. Soc.* **2003**, *125*, 9424 – 9434; c) C. A. Jaska, K. Temple, A. J. Lough, I. Manners, *J. Am. Chem. Soc.* **2004**, *126*, 9776 – 9785.

[8] a) H. C. Kelly, F. R. Marchelli, M. B. Giutso, *Inorg. Chem.* **1964**, *3*, 431 – 437; b) G. E. Ryschkewitsch, *J. Am. Chem. Soc.* **1960**, *82*, 3290 – 3294.

[9] M. E. Bluhm, M. G. Bradley, R. Butterick, U. Kusari, L. G. Sneddon, *J. Am. Chem. Soc.* **2006**, *128*, 7748 – 7749.

[10] H. Nöth, H. Beyer, *Chem. Ber.* **1960**, *93*, 928 – 930.

[11] B. L. Davis, D. A. Dixon, E. B. Garner, J. C. Gordon, M. H. Matus, B. Scott, F. H. Stephens, *Angew. Chem.* **2009**, *121*, 6944 – 6948; *Angew. Chem. Int. Ed.* **2009**, *48*, 6812 – 6816.

[12] M. P. Stracke, G. Ebeling, R. Cataluna, J. Dupont, *Energy Fuels* **2007**, *21*, 1695 – 1698.

[13] L. V. Titov, M. D. Levicheva, *Zh. Neorg. Khim.* **1969**, *14*, 2886 – 2887.

[14] L. V. Titov, M. D. Levicheva, G. N. Dubikhina, *Zh. Neorg. Khim.* **1972**, *17*, 1181 – 1182.

[15] a) R. Custelcean, J. E. Jackson, *Chem. Rev.* **2001**, *101*, 1963 – 1980; b) T. J. Groshens, A. R. Hollins, *Chem. Commun.* **2009**, 3089 – 3091.

[16] The weight loss during the TGA measurement differs from the theoretical calculated value because the liquid products generated by dehydrogenation are carried away in the inert gas stream.

[17] Turbomole 6.0: a) R. Ahlrichs, M. Bär, M. Häser, H. Horn, C. Kölmel, *Chem. Phys. Lett.* **1989**, *162*, 165 – 169; b) F. Weigend, M. Häser, *Theor. Chem. Acc.* **1997**, *97*, 331 – 340; c) M. Kollwitz, J. Gauss, *Chem. Phys. Lett.* **1996**, *260*, 639 – 646.

[18] A. Schäfer, C. Huber, R. Ahlrichs, *J. Chem. Phys.* **1994**, *100*, 5829 – 5835.

[19] G. Rasul, G. K. S. Prakash, G. A. Olah, *Inorg. Chem.* **1999**, *38*, 44 – 47; G. Rasul, G. K. S. Prakash, G. A. Olah, *J. Mol. Struct.* **2007**, *818*, 65 – 70; G. Rasul, G. K. S. Prakash, G. A. Olah, *Inorg. Chem.* **1999**, *38*, 44 – 47.